Characterization of a Cryogenic Fuel Capsule in a Transparent Hohlraum

Rachel Kurchin

The Harley School
Rochester, NY

Advisors: Dr. R. S. Craxton, Mr. M. Wittman

Laboratory for Laser Energetics
University of Rochester
Rochester, NY
November 2008

Abstract

Characterization of a spherical cryogenic fuel capsule in a cylindrical hohlraum is important for indirect-drive inertial-confinement-fusion implosions, as the capsules must be as uniform as possible. Shadowgraphic image analysis techniques developed for spherical capsules have been adapted to evaluate the uniformity of capsules in hohlraums. An existing ray-trace code has been extended to add the hohlraum and predict the apparent outer capsule radius and bright ring radius as functions of angle around the viewing direction. The extended code can also make predictions for capsules that are displaced within the hohlraum. The predictions of the code have been confirmed by data obtained under a microscope using a surrogate capsule (a thick, spherical plastic shell) in a glass hohlraum. By subtracting the predicted distortions from the measurements of the bright ring radius, the uniformity of the inner surface of the capsule can be assessed. The uniformity of capsules in hohlraums can now be evaluated to a degree of accuracy constrained primarily by the uniformity of the hohlraum.

1. Introduction

Fusion is extremely promising as an almost limitless source of energy and is being investigated around the world. It is cleaner and potentially more cost-effective than current nuclear energy sources because it avoids the production of long-lived radioactive waste. Fusion is based upon combining two smaller atoms to make a larger one – the way the Sun creates energy. The fusion reaction generally attempted on Earth proceeds thus:

$$^2H + ^3H \rightarrow ^4He + n,$$

where ^2H is deuterium, the hydrogen isotope with one neutron, ^3H is tritium, the isotope with two neutrons, ^4He is helium, and n is a high-energy neutron. However, this seemingly simple reaction poses many problems because fusion must occur at an extremely high temperature, and it is

difficult to contain the reactants under such extreme conditions.

There are two main techniques being investigated to contain the deuterium and tritium: magnetic confinement and inertial confinement. In magnetic confinement, the deuterium and tritium are maintained in a vacuum chamber at high temperature for long times (seconds and longer) by large magnetic fields. In inertial confinement, high-power laser beams are used to rapidly heat and compress a capsule typically consisting of a thin plastic outer layer and a thick layer of deuterium-tritium (DT) ice. Once the capsule has been compressed, the deuterium and tritium are confined only by their own inertia. Inertial confinement fusion reactions occur much faster than in magnetic confinement, typically finishing on the order of nanoseconds rather than seconds.

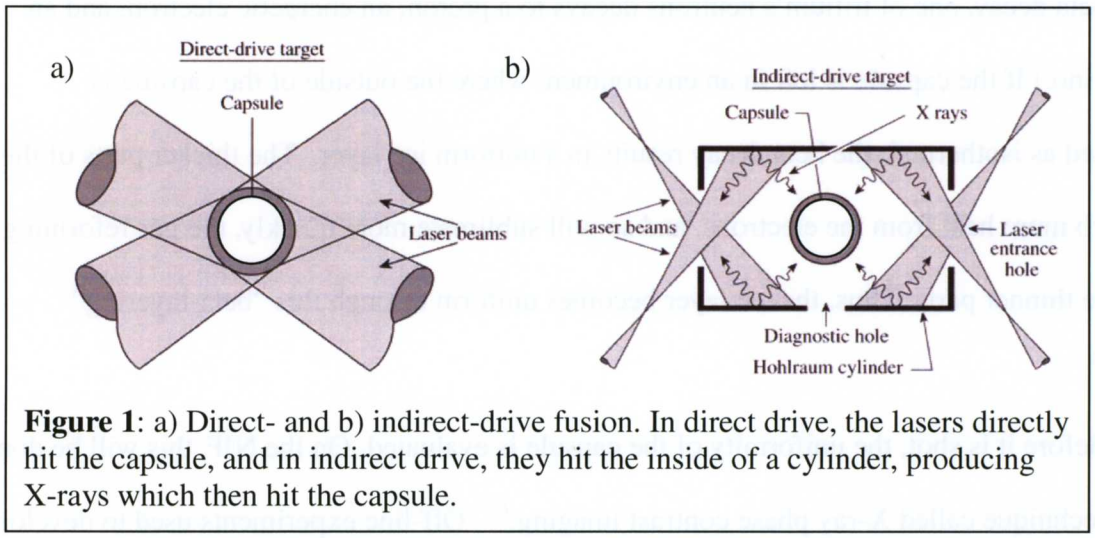

Figure 1: a) Direct- and b) indirect-drive fusion. In direct drive, the lasers directly hit the capsule, and in indirect drive, they hit the inside of a cylinder, producing X-rays which then hit the capsule.

There are two general categories of inertial-confinement fusion: direct drive[1] and indirect drive.[2] In direct drive, the capsule is directly irradiated by the laser beams (see **Figure 1a**), causing the plastic layer to ablate. The reaction force to the ablation compresses the DT fuel forcing it to implode. In indirect drive, the subject of this paper, the lasers irradiate the inside of a cylinder known as a hohlraum. The cylinder produces X-rays, which reflect around the inner surface, eventually hitting the capsule from various directions (see **Figure 1b**). This results in a

more uniform irradiation but lower efficiency because most of the energy is lost to the hohlraum and thus not transferred to the capsule.[2] The National Ignition Facility[3] (NIF), a large laser due to be completed in 2010, will use indirect drive. Inertial confinement fusion requires the maximum possible capsule uniformity since thinner parts of the capsule implode more quickly, magnifying nonuniformities.

Typical cryogenic capsules[4] start as only the plastic shell. On the NIF, they will be filled with DT gas using a very small "fill tube" attached to the capsule. The fill tube is also attached to a reservoir of DT and is sealed off once the desired amount is inserted in the capsule. Next, the shells are gradually cooled for the ice layer to form. The naturally formed ice layer is never uniform, but since tritium is radioactive, the electrons produced by its beta decay will heat the ice. (In beta decay, one of tritium's neutrons decays to a proton, an energetic electron, and an antineutrino.) If the capsule is left in an environment where the outside of the capsule is maintained as isothermal, the beta decay results in a uniform ice layer. The thicker parts of the ice absorb more heat from the electrons, and so will sublimate more quickly, the gas reforming as ice on the thinner parts. Thus, the ice layer becomes uniform through this "beta-layering" process.[5]

Before it is shot, the uniformity of the capsule is evaluated. On the NIF, this will be done using a technique called X-ray phase contrast imaging.[6,7] Off-line experiments used to develop the layering process for capsules in hohlraums will use both X-ray phase-contrast imaging and shadowgraphy. Shadowgraphy consists of passing light through the capsule, taking an image of the capsule, and using patterns in the image to determine the layer uniformity. Shadowgraphy has been used extensively in the past to characterize cryogenic capsules; a direct comparison between shadowgraphy and X-ray phase-contrast imaging will allow a valuable cross calibration

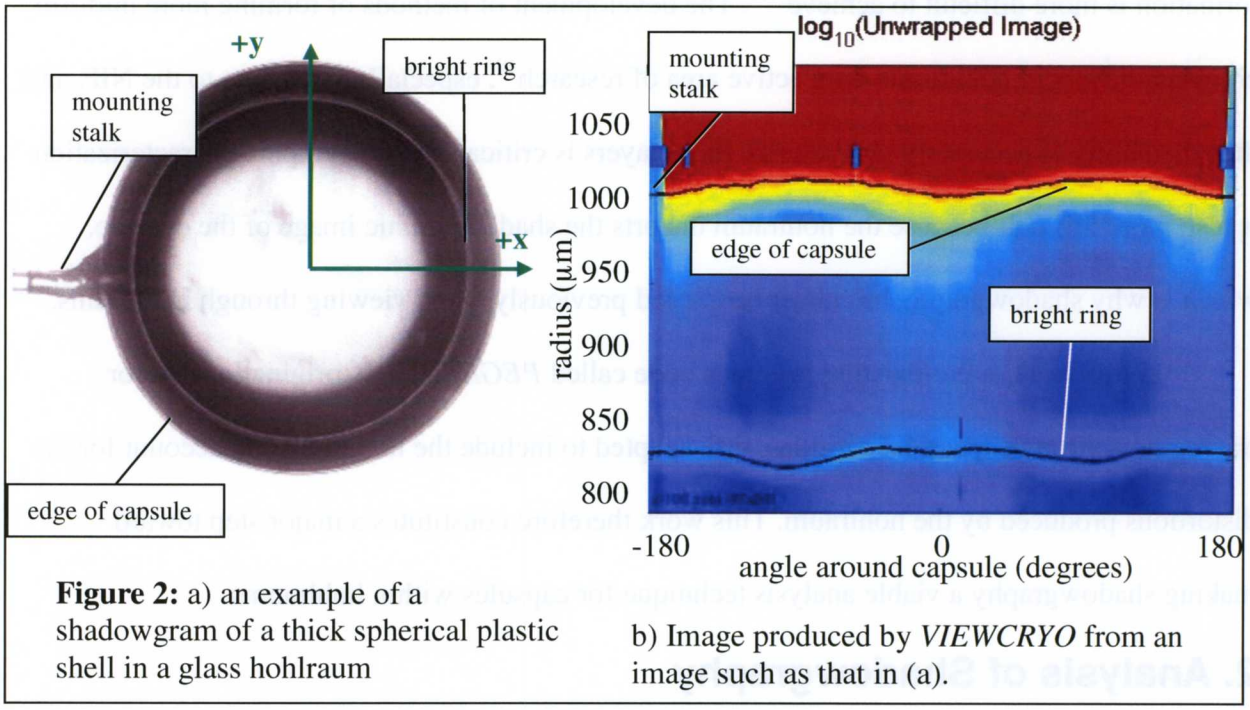

Figure 2: a) an example of a shadowgram of a thick spherical plastic shell in a glass hohlraum b) Image produced by *VIEWCRYO* from an image such as that in (a).

of the two techniques.

An example of a shadowgram can be seen in **Figure 2a**, in which a plastic shell (rather than a DT layer) is used as a surrogate to test the effect of a hohlraum on shadowgraphy before a cryogenic experiment is attempted. In the image, the light regions outside the capsule edge and in the center correspond to the light source being transmitted without much loss. The darker areas are where the rays are blocked by the capsule. While the rings in the image (the outer edge and bright ring) appear circular, they contain deviations from constant radius that can be directly used to evaluate the capsule nonuniformity. An analysis program called *VIEWCRYO*[8], used in the experimental part of this work, produces an image such as that in **Figure 2b** from a shadowgram, showing the variations in radius of these two rings. The curves seen in **Figure 2b** are typical of the distortions created by the hohlraum, and to evaluate the uniformity of a capsule, they must be accounted for.

When the capsule is layered inside a hohlraum, as must be done for indirect drive, it is more difficult to layer it evenly because the isothermal environment required for uniform layer

formation is more difficult to achieve[9,10]. The development of methods of forming more uniform cryogenic layers in hohlraums is an active area of research[10], especially important to the NIF, and thus the ability to accurately characterize these layers is critical. Shadowgraphic characterization is also more difficult because the hohlraum distorts the shadowgraphic image of the capsule, which is why shadowgraphy has never been used previously when viewing through hohlraums.

In this work, a pre-existing ray-trace code called *PEGASUS*,[11,12] originally used for tracing rays through spherical capsules, was adapted to include the hohlraum and account for the distortions produced by the hohlraum. This work therefore constitutes a major step toward making shadowgraphy a viable analysis technique for capsules within hohlraums.

2. Analysis of Shadowgraphy

The origin of the features visible in **Figure 2a** can be explained with **Figure 3**. This figure shows ray trajectories through a spherical glass capsule placed inside a cylindrical hohlraum. A-rays pass directly through all surfaces of the hohlraum and capsule, forming the light region in the center of **Figure 2a**. B-rays (shown in **Figure 3a**) are reflected off the inner ice surface and when projected back appear to come from a very small region known as a bright ring[13]. C-rays do not hit the capsule, thus forming the lightest region outside the image of the capsule. Note that the C-ray path length increases with increased distance y from the horizontal axis, as in a (concave) divergent lens which is thicker further from the center, so the C-rays emerge diverging. U- rays (shown in Figure 3b) are similar to B-rays, but reflect off the inner ice surface from the inside. It should be noted that the ray traces in **Figure 3** do not include the full range of rays that would pass through the target. Some C- and A-rays are omitted for clarity, and the B- and U-rays are omitted if their angles of deflection upon emergence are too great to be collected by the lens. The bright ring formed by B rays has been used consistently as the main

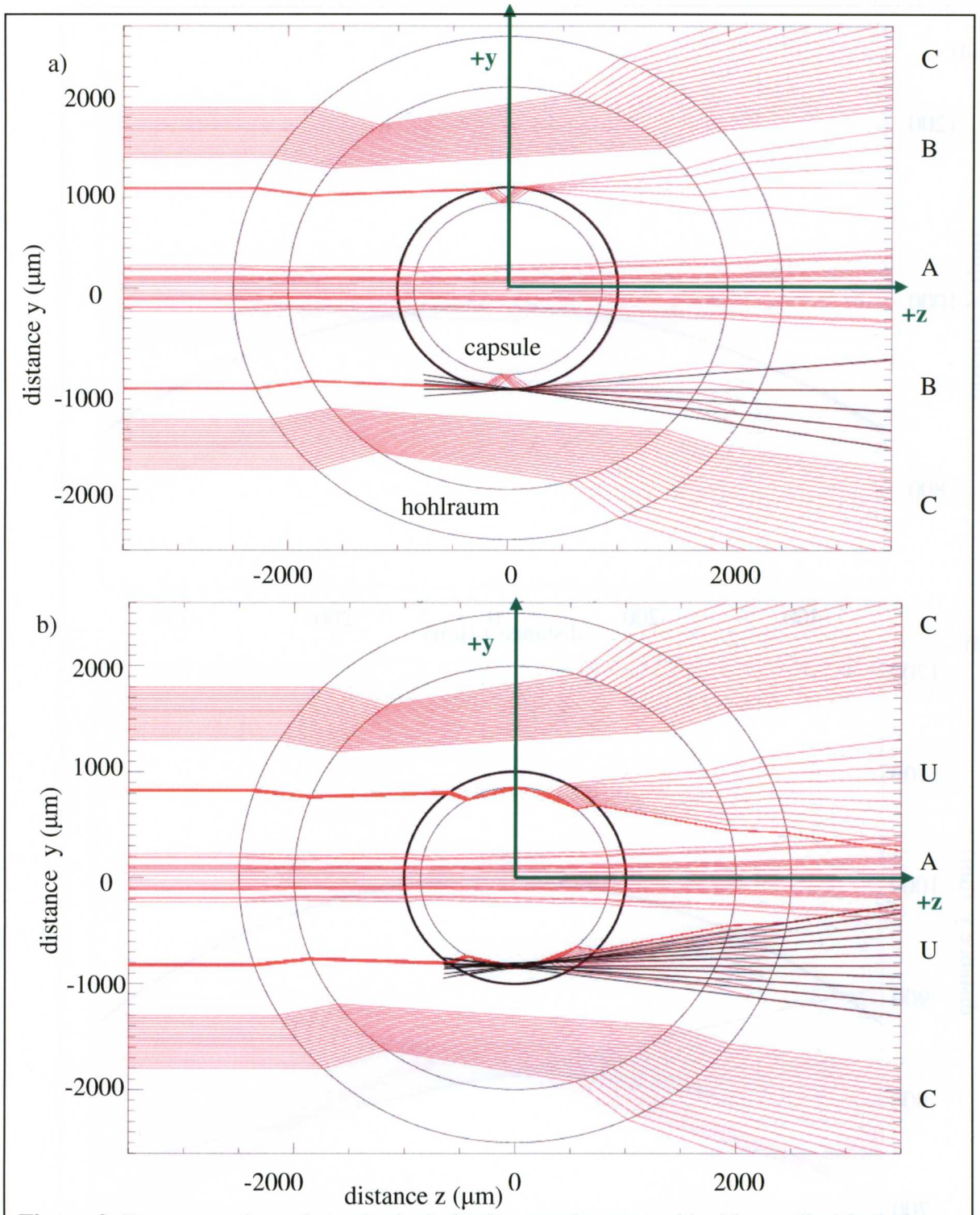

Figure 3: Ray traces through a spherical plastic capsule centered inside a cylindrical glass hohlraum, showing the different types of rays refracting/reflecting through the setup. Bright rings are formed from the B rays (shown in **a**) and the U rays (shown in **b**); the bottom half of each vertically symmetrical trace shows these rays back-projected in black, demonstrating the small regions that the rays appears to come from. Note that the positive x-axis goes into the page.

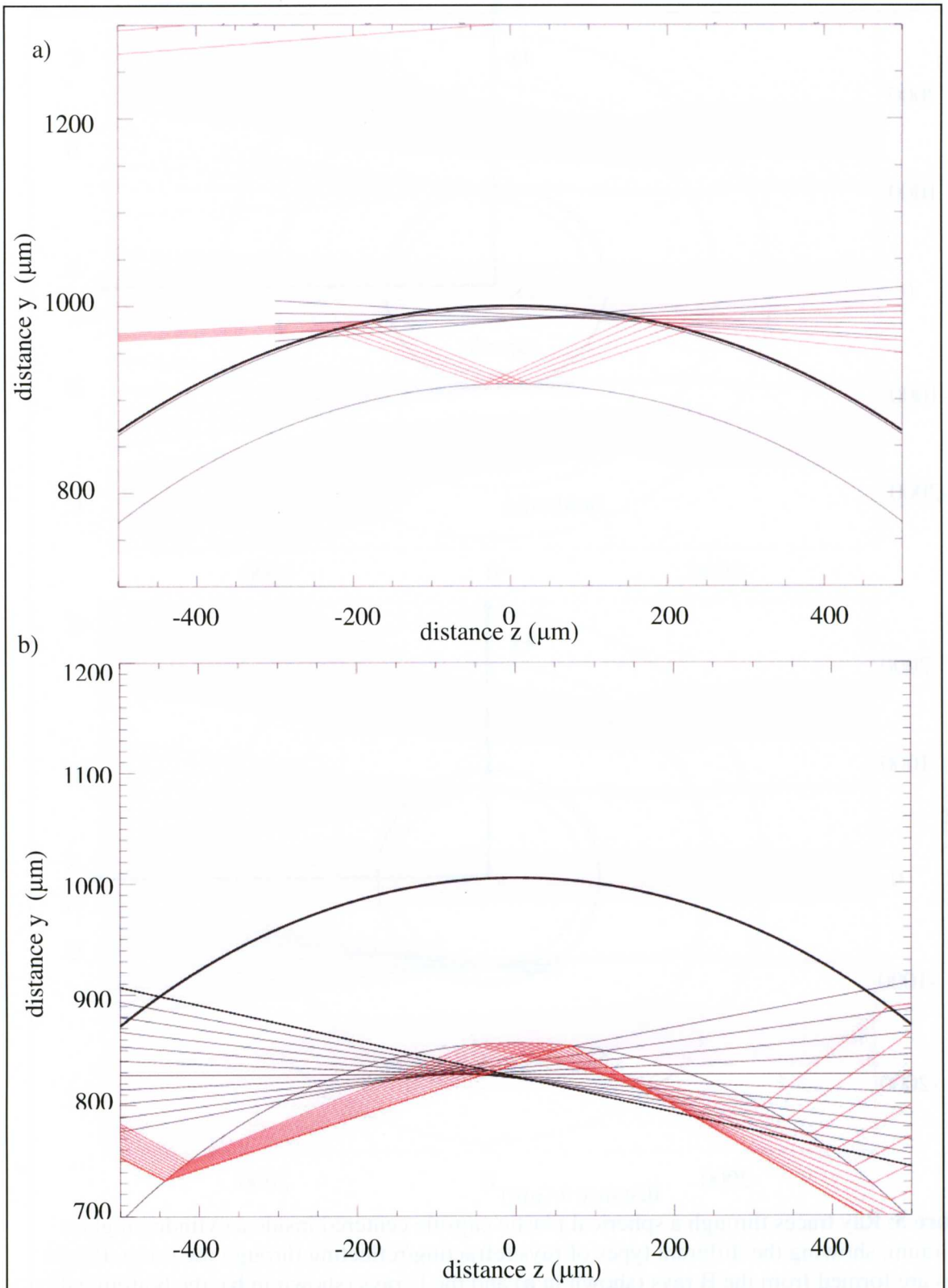

Figure 4: Zoom on the caustic regions corresponding to **Figure 3**. a) B-rays, b) U-rays The black lines indicate back-projected rays.

indicator of cryogenic layer uniformity[8,13,14]. The radius of the ring is not equal to the actual inner ice surface radius, but it is a reliable indicator of nonuniformity nonetheless because changes in the inner surface radius correspond closely to changes in the ring radius

In this experiment, the plastic surrogate capsule had a different refractive index and thickness than a DT capsule, so the rays behave slightly differently. While the ring formed by the B rays is the most visible for cryogenic capsules, the most visible ring for the surrogate capsule is formed by U-rays. This can be seen in Figure 4, which shows blowups of (a) the backprojected B rays and (b) the backprojected U rays. When the microscope used to view the capsule is focused on the point on the caustic where the rays cross (just to the right of z=0 for B rays and just to the left for U-rays), a bright ring is seen. From **Figure 4a**, the place where the B-rays appear to come from in the surrogate capsule is too close to the edge of the capsule to be distinguished from it. Thus the U rays were used. They have never before been used for the analysis, although they have been observed[8], so a model for them was added to the code. As can be seen in **Figure 4b**, the rays, when projected backwards, form a distinct ring far enough inwards from the capsule edge to be accurately imaged and analyzed.

3. Code Development

The code *PEGASUS*, which included routines for the refraction of rays through planes and spherical surfaces using Snell's Law, was modified to model the distortion introduced by the hohlraum by adding a routine for refraction through cylindrical surfaces. The code is written to be as general as possible, and thus includes many different parameters describing the objects through which the rays travel. In addition to the radius and refractive index of each layer of the capsule and hohlraum, the position of the sphere within the cylinder can be modified such that the code can also be used for capsules that aren't perfectly centered. The direction of the cylinder

axis can also be modified. In addition, a U-ray model was built and added to the code to model surrogate capsules.

The bright ring and outer radius of the capsule are calculated using a binary search algorithm, as indicated in **Figure 5**, for each angle θ in the image (see **Figure 6**). The bright ring radius at each angle is defined by the B-ray (or U-ray) which enters and exits the hohlraum horizontally. The outer radius at each angle is defined by the C-ray that just misses the capsule as it goes through the inside of the hohlraum. To find the bright ring radius, the binary search starts with two arbitrary radii and gradually refines its calculations based on whether the rays emerge too high or too low. To find the outer radius, it instead tests for whether the rays hit or miss the capsule. The user can specify the accuracy by choosing how many passes the search routine should make. The code typically calculates these radii for 360 angles θ around the capsule image (see **Figure 6**) and graphs them.

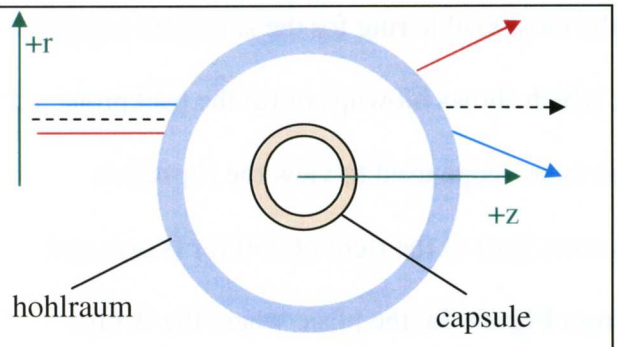

Figure 5: Schematic illustrating how the bright ring radius is found. A ray launched at the hohlraum/capsule combination from too large a radius (blue) will emerge too low, and vice versa (red). The ray that enters and exits horizontally (dashed black) is found using a binary search and defines the bright ring radius.

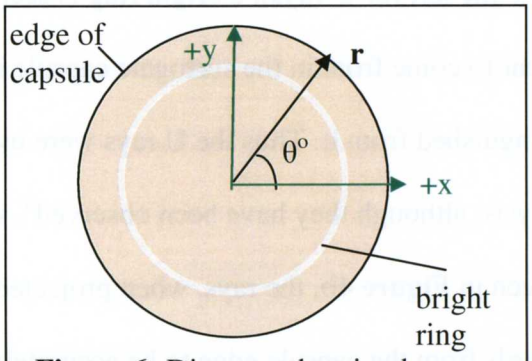

Figure 6: Diagram showing how the angle θ around the capsule image is defined. At each value of θ, the radii of the bright ring and the edge of the capsule are calculated.

4. Experimental Results

A) Experimental Setup

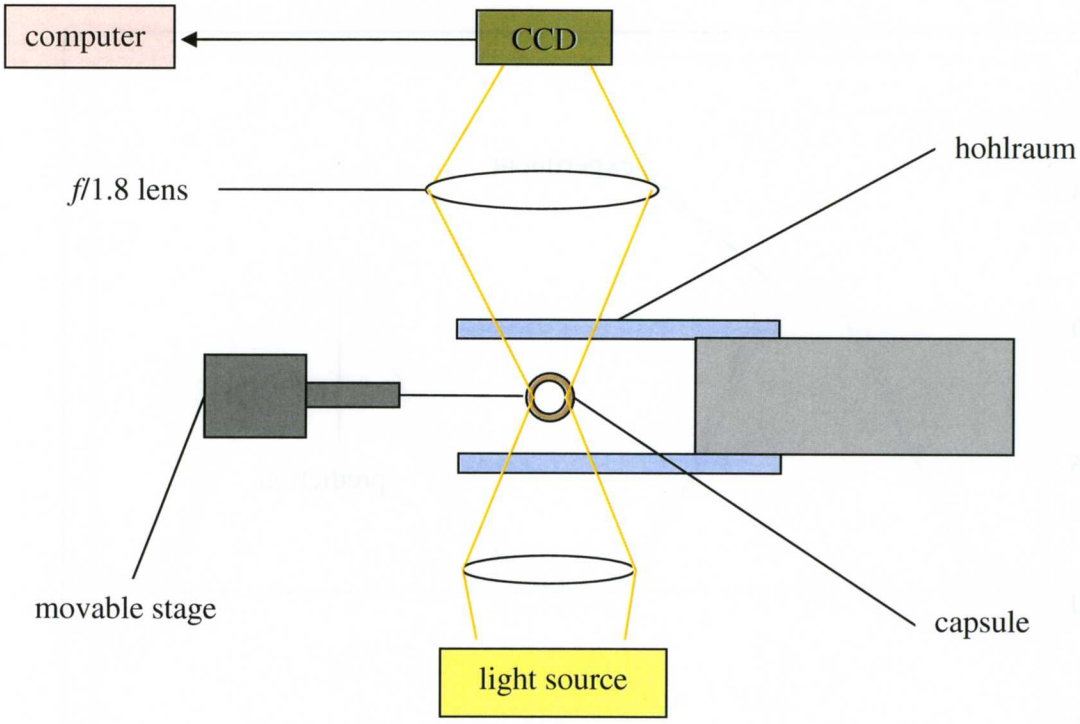

Figure 7: Schematic of the experimental apparatus. The capsule is illuminated by a light source and viewed using a microscope with an f/1.8 lens. An image of the capsule is formed on a CCD camera and stored in the computer. The position of the capsule can be adjusted in three dimensions.

A schematic of the experimental apparatus is shown in **Figure 7.** The plastic capsule was mounted on a stalk and manipulated on a movable stage adjustable in three dimensions. The hohlraum was mounted across from the capsule and the capsule could be moved in and out of the hohlraum. The capsule/hohlraum setup was viewed using a traveling microscope connected to a readout giving coordinates of the locations of the capsule and hohlraum in three dimensions, with uncertainties of ±10 μm in the z-axis (toward and away from the lens) and ±5 μm in the x- and y-axes. Photographs of the capsule were taken with a digital camera (with a resolution of ~2 μm/pixel) attached to the microscope and then stored in a computer. The shadowgram in **Figure 2** was obtained using this setup.

B) Measurements of the Outer Radius

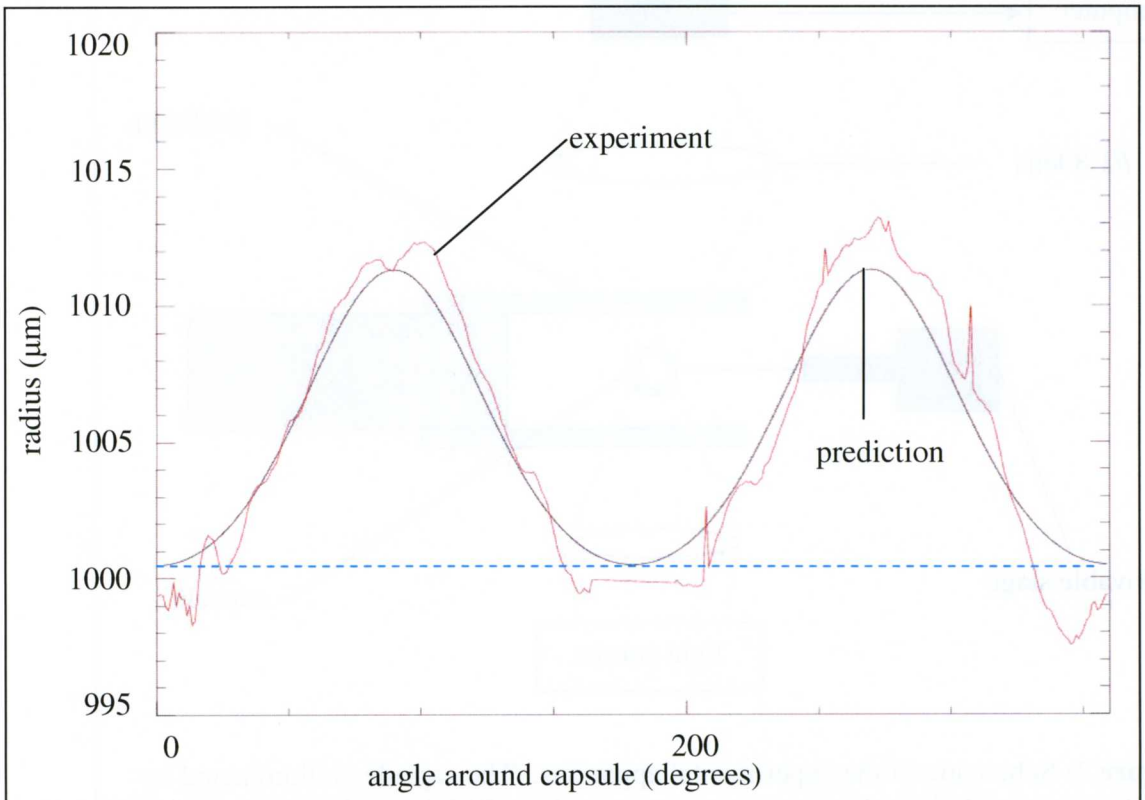

Figure 8: Predicted and measured outer radius of a capsule viewed through a hohlraum as functions of angle. The blue dotted line represents the actual (average) capsule radius.

Code predictions and measured data for the outer radius of the capsule as a function of the angle around the capsule are shown in **Figure 8**. The code predicted a pattern with two maxima and two minima and the measured data supported these predictions very well. This pattern is in accordance with expectations. The maximum distortion is predicted at 90° and 270°, where the hohlraum surface is tipped furthest away from the ray path, and no distortion is predicted at 0° and 180°, where looking through the hohlraum is analogous to looking through a plane parallel plate and should cause no distortion. The flat portion of the experimental graph around 180° appears because *VIEWCRYO* cannot locate the edge of the capsule due to the presence of the mounting stalk (see **Figure 2a**) and ignores this data.

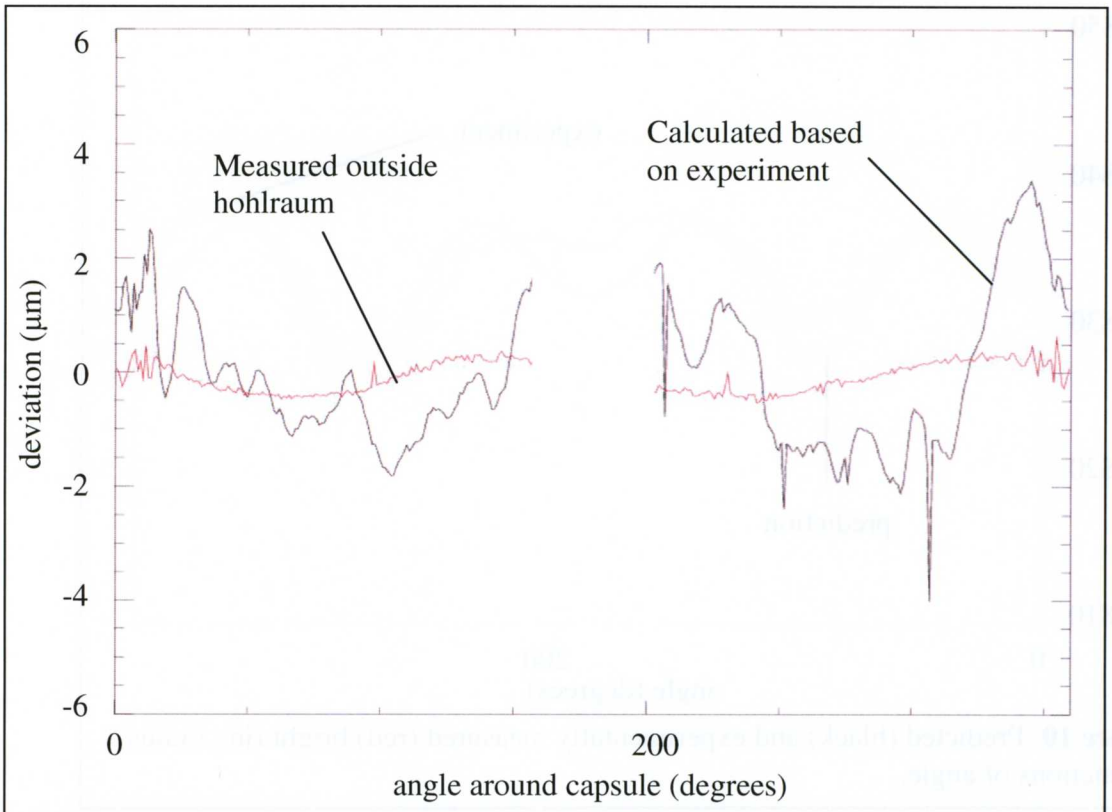

Figure 9: Calculated and measured capsule nonuniformity, with data omitted for the portion interfered with by the stalk. The calculated nonuniformity is found by subtracting the two curves shown in **Figure 8**.

By subtracting the predictions from the measured data, effectively "canceling out" distortions from the hohlraum, one can obtain a graph of the nonuniformity of the capsule's outer surface. This is shown by the black line of **Figure 9**. However, when this was compared with a measurement of the capsule's outer radius outside the hohlraum, shown as the red line in **Figure 9**, it was seen to be slightly inaccurate (±2 μm in a capsule radius of 1000 μm). This is probably due to the nonuniformity of the hohlraum, which is not known and could not be taken into account in the original calculation.

C) Measurements of the Bright Ring Radius

A graph comparing predictions and measured data for the bright ring radius is shown in

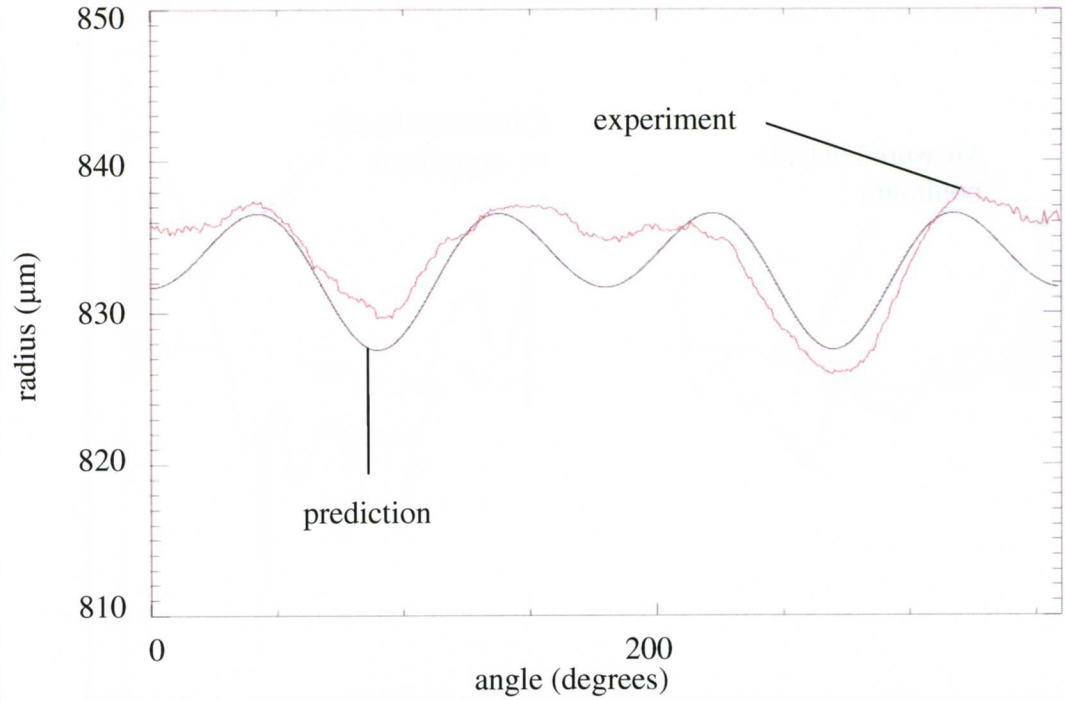

Figure 10: Predicted (black) and experimentally measured (red) bright ring radius as functions of angle.

Figure 10. In contrast to **Figure 8**, the code predicted a four-lobe pattern, which was unexpected. The data support the predicted trend fairly closely.

The difference between the two curves of **Figure 10** was plotted as the black curve in **Figure 11** providing a graph indicating the nonuniformity of the bright ring radius. The red curve represents the measured nonuniformity outside the hohlraum. Again, the lack of correlation is probably due to the nonuniformity of the hohlraum. It should be noted that the measured nonuniformity of the bright ring radius outside the hohlraum is greater than that of the outer radius (red curve of **Figure 9**). This could be because the inner surface is less uniform than the outer surface, but it is more likely because the U-rays travel through the nonuniform outer surface of the capsule and also sample the inner surface in three places, resulting in several nonuniformities adding up to an overall error of ±4 μm.

When similar experiments are performed with cryogenic capsules using the B rays, this

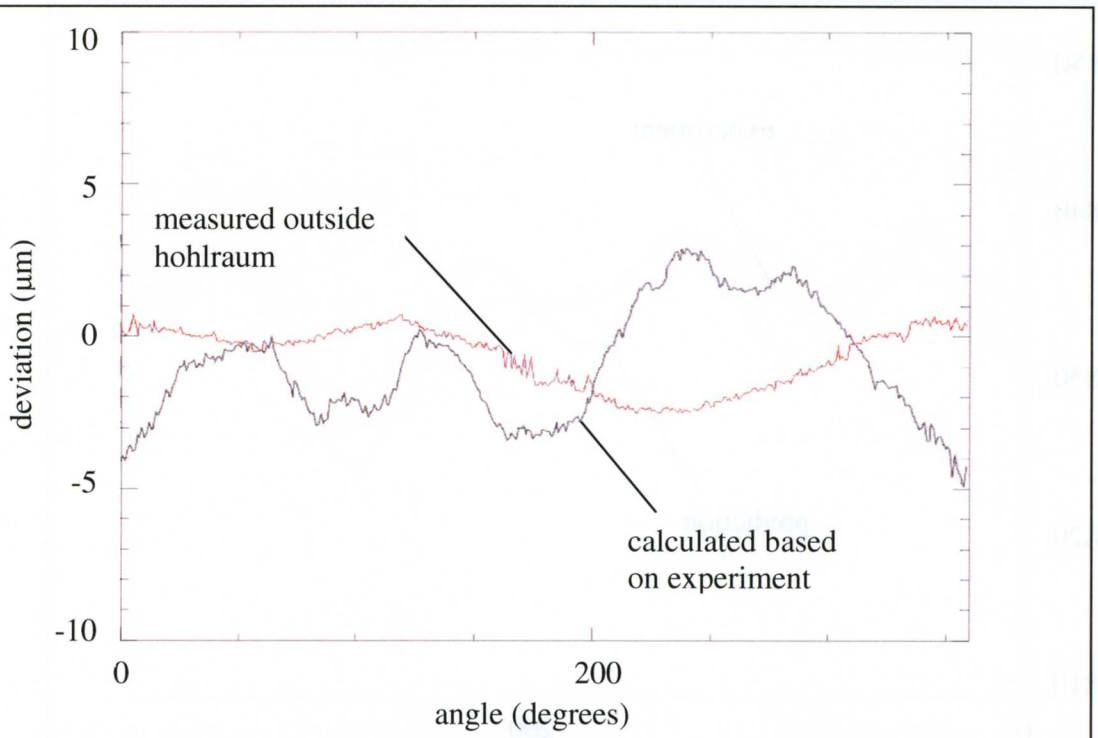

Figure 11: Calculated and measured nonuniformity of the bright ring as functions of angle. The calculated nonuniformity was obtained by subtracting the two curves shown in **Figure 10**.

effect should be reduced because the B-rays do not sample as many surfaces as do the U-rays. In particular, they only sample the inner surface in one place. More importantly, tight specifications must be imposed on the uniformity of the hohlraum if accurate data are to be obtained for both the outer and bright ring radii.

D) Displaced Capsule

The code was also tested for a capsule that was off-center within the hohlraum. The experimental setup was the same as before but the capsule was intentionally displaced by a known amount in the y-direction (the x-axis being along the cylinder and displacement along it therefore irrelevant). For a displacement of 100 μm, much greater than the positioning accuracy of the capsule, the data matched predictions as well as they did for the centered capsule (see **Figure 12**). Similar results were obtained for displacement in the z-direction. Having this

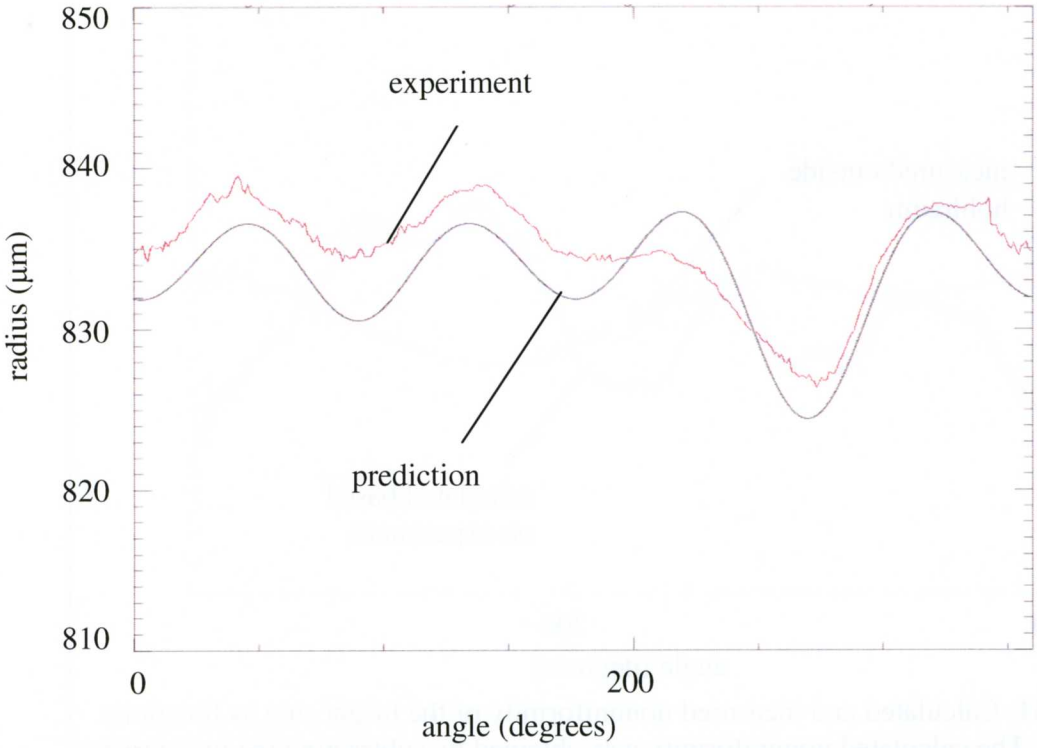

Figure 12: Predicted and experimentally measured bright ring radius for a capsule displaced 100 μm in the y direction.

capability in the code is important because it will allow detection of and compensation for small errors introduced by capsule mispositioning.

In **Figure 12**, a small adjustment of the (R, θ) values produced by the code was necessary to compare with *VIEWCRYO*, which was not designed for use with a hohlraum and therefore finds the center slightly incorrectly as the centroid of the image. In a hohlraum setup with a capsule displaced in the y-direction this does not correspond to the center because one side will necessarily be distorted more due to the hohlraum. The details of this adjustment are given in the Appendix.

5. Conclusion

Uniform DT cryogenic layers are of critical importance for the hohlraum targets proposed for the NIF. Layering techniques for capsules within hohlraums are currently under development.

A code was developed to address the problem that shadowgraphy could not previously be used to measure the uniformity of a capsule in a hohlraum. The code calculates the distortion introduced by the hohlraum to the image of the capsule, enabling this to be compensated for.

The predictions of the code were tested using a plastic surrogate capsule inside a glass hohlraum. Experimental data confirmed the predicted pattern for the outer radius as well as the unexpected four-lobed pattern predicted for the bright ring radius. The code enabled the nonuniformity of the outer surface of the capsule to be calculated very accurately (±2 μm in a radius of 1000 μm) and the bright ring to a lesser degree of accuracy (±4 μm). The accuracy of both was limited primarily by the uniformity of the hohlraum, and therefore demonstrated the necessity of more uniform hohlraums for future experiments. The bright ring measurements were also affected by the rays sampling many imperfect surfaces, producing deviations that were too large. However, when similar work is done with cryogenic capsules, this should not be an issue because the B-rays will be used, and they only sample the inner DT ice layer at one point. The results of this work show that shadowgraphy can indeed be used to evaluate the uniformity of capsules in hohlraums.

6. Appendix

Because *VIEWCRYO* was designed for shadowgrams of unenclosed capsules rather than capsules in hohlraums, its algorithm for finding the center of the capsule image consistently calculated it incorrectly for images of capsules displaced in the y direction. This is because *VIEWCRYO* calculates the center as the centroid of the capsule edge (the average x,y values), which will fail for the y value because the hohlraum-induced distortions at the top and bottom of the image are different. Thus, in order for a viable comparison to be made, *PEGASUS* has to compensate for this by altering its predictions such that they are based on where *VIEWCRYO*

would calculate the center to be. It does this by finding the centroid, and then recalculating the radius and angle values for each data point.

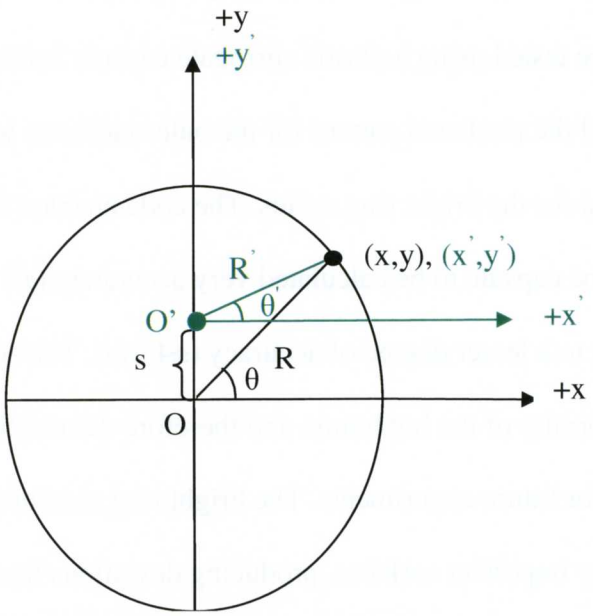

Figure 13: Diagram demonstrating how the R(θ) curves calculated by *PEGASUS* are adjusted to match the R'(θ') curves generated by *VIEWCRYO* based on the primed (green) coordinate system. The distance s is exaggerated for clarity.

Mathematically, this proceeds as follows (see **Figure 13**): The origin O' of the *VIEWCRYO* coordinate system (x', y'), is shifted a distance *s* in the y direction. The x coordinate does not change. Thus:

$$x'=x$$

$$y'=y-s.$$

For any point along the capsule edge for which R has been calculated, its coordinates can be expressed as:

$$(x,y) = (R\cos\theta, R\sin\theta)$$

or, in the new coordinate system, as:

$$(x',y') = (R'\cos\theta', R'\sin\theta')$$

Using the above definitions of (x', y'), R' and θ' can now be found as

$$R' = \sqrt{(x'^2+y'^2)}$$

$$\theta' = \tan^{-1}(y'/x').$$

R' and θ' are then used to generate new graphs that can be viably compared to *VIEWCRYO*'s data. The same process occurs for the bright ring data.

7. Acknowledgments

I would like to extend my heartfelt gratitude to Dr. R. Stephen Craxton for being my endlessly patient theoretical advisor, to Mr. Mark Wittman, my experimental advisor, for patiently explaining the experimental process and helping me along the way, and to Dr. Dana Edgell for his help in using the *VIEWCRYO* program for my project.

8. References

[1] J. Nuckolls, *et al.*, "Laser Compression of Matter to Super-High Densities: Thermonuclear (CTR) Applications", *Nature*, **239**, 139 (1972)

[2] J.D. Lindl, "Inertial Confinement Fusion", Springer-Verlag, New York (1998)

[3] E. M. Campbell, W. J. Hogan, "The National Ignition Facility – Applications for Inertial Fusion Energy and High-Energy-Density Science," *Plasma Physics Control. Fusion*, **41**, B39 (1999)

[4] D. R. Harding, *et al.*, "Producing Cryogenic Deuterium Targets for Experiments on OMEGA", *Fusion Science and Technology*, **48**, 1299, (2005)

[5] A. J. Martin, R. J. Simms, R. B. Jacobs, "Beta energy driven uniform deuterium-tritium ice layer in reactor-size cryogenic inertial fusion targets", *J. Vac. Sci. Technol.*, **A 6 (3)**, 1885, (1988)

[6] D. S. Montgomery, A. Nobile, P. J. Walsh, "Characterization of National Ignition Facility cryogenic beryllium capsules using x-ray phase contrast imaging", *Review of Scientific Instruments*, **75**, 3986, (2004)

[7] B. J. Kozioziemski, *et al.*, "Quantitative characterization of inertial confinement fusión capsules using phase contrast enhanced x-ray imaging", *Journal of Applied Physics*, **97**, 063103 (2005)

[8] D. H. Edgell, *et al.*, "Three-Dimensional Characterization of Cryogenic Target Ice Layers Using Multiple Shadowgraph Views", *Fusion Science and Technology*, **49**, 616 (2006)

[9] B.J. Kozioziemski, *et al.*, "Infrared heating of hydrogen layers in hohlraums", *Fusion Science and Technology* **41**, 296 (2002).

[10] J.D. Moody, *et al.*, "Status of cryogenic layering for NIF ignition targets", *J. Physics* **112**, 032064 (2008).

[11] S. Jin, "A Ray-Tracing Model for Cryogenic Target Uniformity Characterization," 2002 Summer High School Research Program at the University of Rochester's Laboratory for Laser Energetics. LLE Report No. 329.

[12] G. Balonek, "How Good is the Bright Ring Characterization for Uniformity of Deuterium Ice Layers within Cryogenic Nuclear Fusion Targets?", 2004 Summer High School Research Program at the University of Rochester's Laboratory for Laser Energetics. LLE Report No. 337.

[13] D. N. Bittner, *et al.*, "Forming Uniform HD Layers in Shells Using Infrared Radiation", *Fusion Technology*, **35**, 244 (1999)

[14] J.A. Koch, *et al.*, "Numerical raytrace verification of optical diagnostics of ice surface roughness for inertial confinement fusion experiments", *Fusion Science and Technology*, **43**, 55 (2003)